



Identifying Tolerable Wavefront Aberrations as a Function of the Pinhole Diameter of a Spatial Filter in a Nulling Interferometer

Semester Project

Author
Philipp A. Huber

Supervisor
Dr. Adrian Glauser

June 2021
Institute for Particle Physics and Astrophysics
Department of Physics
ETH Zurich

Abstract

This is the abstract.

Acknowledgements

Contents

1	Introduction	1
2	Theory	2
2.1	Aberrated Wavefronts	2
2.2	Fraunhofer Diffraction of Aberrated Wavefronts	3
2.3	Spatial Filtering of Aberrated Wavefronts	5
2.4	Null Depth	5
2.5	Throughput	6
3	Methodology	7
3.1	Normalization	7
4	Results	8
5	Discussion	9
6	Conclusion	10
	References	11
	Appendices	12

List of Figures

2.1	Illustration of the setup with one aperture.	4
2.2	Illustration of the $4f$ -system setup.	6

List of Tables

1 Introduction

2 Theory

2.1 Aberrated Wavefronts

Zernike Polynomials

Wavefront errors can be modeled using Zernike polynomials. A certain Zernike polynomial is specified by two indices $n, m \in \mathbb{N}_0$ with $n \geq m$. They can be expressed in Cartesian coordinates as

$$Z_n^m(\rho, \theta) = \text{sign}(m) \sqrt{\frac{2(n+1)}{1+\delta_{m0}}} R_n^{|m|}(\rho) \begin{cases} \cos m\theta & m \geq 0 \\ \sin |m|\theta & m < 0, \end{cases} \quad (2.1)$$

where δ_{m0} is the Kronecker delta function. The radial part is given by

$$R_n^m(\rho) = \begin{cases} \sum_{k=0}^{\frac{n-m}{2}} \frac{(-1)^k (n-k)!}{k! (\frac{n+m}{2}-k)! (\frac{n-m}{2}-k)!} \rho^{n-2k} & n-m \text{ even} \\ 0 & n-m \text{ odd} \\ 1 & \rho = 1 \end{cases} \quad (2.2)$$

with $\rho = r/r_{\max}$ the normalized radial coordinate. The normalization of the radial coordinate results in the units of the Zernike polynomials to be unity.

Wavefront Errors

Wavefront errors can then be modeled as a sum of multiple Zernike polynomials, each preceded by a coefficient z_n^m specifying the contribution of the term, i. e.

$$\Delta W(\rho, \theta) = \sum_{n,m} z_n^m Z_n^m(\rho, \theta). \quad (2.3)$$

Note that the coefficients and, as such, also $\Delta W(\rho, \theta)$ have of units length. Equation (2.3) describes the deviation of the wavefront from a perfect wavefront. The root mean

square σ of the wavefront error can then be expressed as (Patil et al., 2014)

$$\sigma = \overline{\Delta W^2} - (\overline{\Delta W})^2 \quad (2.4)$$

$$= \left[\frac{1}{\pi} \int_0^{2\pi} \int_0^1 \Delta W^2(\rho, \theta) \rho d\rho d\theta - \frac{1}{\pi^2} \left(\int_0^{2\pi} \int_0^1 \Delta W(\rho, \theta) \rho d\rho d\theta \right)^2 \right]^{1/2} \quad (2.5)$$

$$= \left[\sum_{n,m} (z_n^m)^2 \right]^{1/2}, \quad (2.6)$$

where in (2.6) we have used the orthogonality relations of the Zernike polynomials. In the following, the wavefront errors and Zernike polynomials will be expressed in Cartesian coordinates u, v by introducing

$$\rho = \frac{\sqrt{v^2 + u^2}}{\sqrt{u_{\max}^2 + v_{\max}^2}}, \quad (2.7)$$

$$\theta = \arctan2(u, v). \quad (2.8)$$

Amplitude of an Aberrated Wavefront

Thus, the amplitude of a monochromatic, spherical wavefront at time t , at distance r from its source and subject to a wavefront error $\Delta W(u, v)$ is given by

$$E_{\text{spherical}}(t, r, u, v) = \frac{E_0}{r} e^{\frac{2\pi i}{\lambda}(ct - r - \Delta W(u, v))}. \quad (2.9)$$

where λ is the wavelength, c the speed of the wave and E_0 the initial amplitude. Note that an ideal wavefront can be modeled similarly simply by setting $\Delta W(u, v)$ to zero.

2.2 Fraunhofer Diffraction of Aberrated Wavefronts

Essentially, the following will be a derivation of Fraunhofer diffraction for the case of an aberrated wavefront. If planar waves hit an aperture, the aperture itself can be interpreted as the source of a wavefront with the amplitude given by (2.9). Consider the setup illustrated in Figure 2.1. To calculate the electric field at a point $P(x, y, z)$ after such an aperture, the following manipulations will become useful. The distance R from the center of the aperture to the point P can simply be written as

$$R = \sqrt{x^2 + y^2 + z^2}. \quad (2.10)$$

For the distance of the infinitesimal surface element dS to point P we find

$$r = \sqrt{z^2 + (x - u)^2 + (y - v)^2} \quad (2.11)$$

$$= R \left(1 - \frac{2(ux + vy)}{R^2} \right)^{1/2} \quad (2.12)$$

$$\approx R \left(1 - \frac{ux + vy}{R^2} \right) \quad (2.13)$$

$$\approx R, \quad (2.14)$$

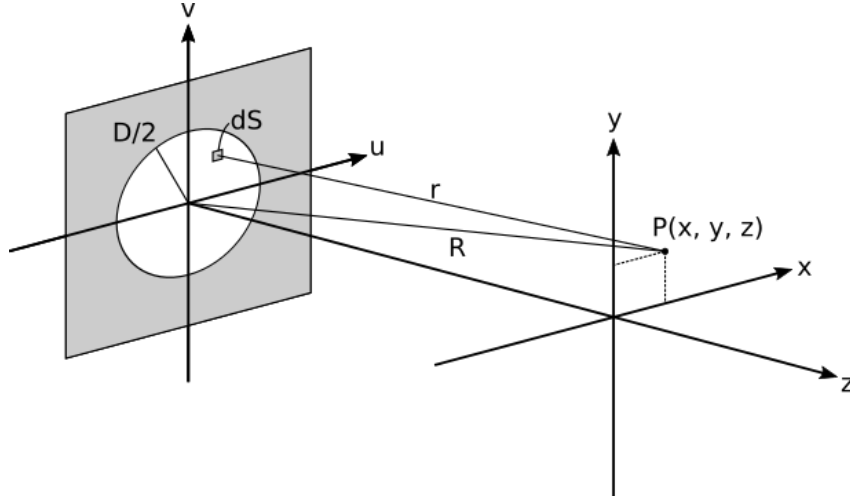


Figure 2.1: Illustration of the setup with one aperture.

where in (2.12) we have used $R \gg D/2$, in (2.13) we have performed a Taylor series expansion and only kept the two first terms and in (2.14) we have assumed that $R \gg x, y$.

The amplitude of the electric field at point $P(x, y, z)$ after the aperture, originating from the surface element dS within the aperture can now be calculated as

$$dE(t, r, u, v) = E_{\text{spherical}}(t, r, u, v) du dv \quad (2.15)$$

$$\approx \frac{E_0}{R} e^{\frac{2\pi i}{\lambda} (ct - R + \frac{ux+vy}{R} - \Delta W(\rho, \theta))} du dv \quad (2.16)$$

$$\approx \underbrace{\frac{E_0}{R} e^{\frac{2\pi i}{\lambda} (ct - R)}}_{\approx \text{const.} \equiv A_0} e^{\frac{2\pi i}{\lambda} (\frac{ux+vy}{R} - \Delta W(u, v))} du dv, \quad (2.17)$$

where in (2.16) we have replaced the r in the denominator of $E(t, r, u, v)$ by (2.14) and the one in the exponential by (2.13) and in (2.17) we have simply rearranged the equation and defined A_0 . Note that $A_0 \approx \text{const.}$ if we assume that $R \approx \text{const.}$ and average over time t . Integrating now (2.17) over the aperture will yield the amplitude of the electric field. For convenience, we can introduce the aperture function

$$A(u, v) = \begin{cases} A_0, & \text{if } (u, v) \in \text{aperture} \\ 0, & \text{else} \end{cases} \quad (2.18)$$

with

$$A_0 \equiv \frac{E_0}{R} e^{\frac{2\pi i}{\lambda} (ct - R)} \approx \text{const.} \quad (2.19)$$

and then simply integrate from minus infinity to plus infinity. For a circular aperture of diameter D , for instance, the aperture function can be written as

$$A(u, v) = A_0 \Theta \left(\frac{D}{2} - \sqrt{u^2 + v^2} \right) \Theta \left(\sqrt{u^2 + v^2} \right), \quad (2.20)$$

where Θ is the Heaviside step function. The amplitude of the electric field at point P is thus given by

$$E(x, y) \approx \int_{-\infty}^{\infty} \int_{-\infty}^{\infty} A(u, v) e^{\frac{2\pi i}{\lambda} \left(\frac{ux+vy}{R} - \Delta W(u, v) \right)} du dv. \quad (2.21)$$

Moving now to the frequency domain by introducing

$$k_x \equiv \frac{2\pi}{\lambda R} x, \quad (2.22)$$

$$k_y \equiv \frac{2\pi}{\lambda R} y \quad (2.23)$$

will simplify things a lot. Equation (2.21) will become

$$E(k_x, k_y) \approx \int_{-\infty}^{\infty} \int_{-\infty}^{\infty} A(u, v) e^{\frac{-2\pi i}{\lambda} \Delta W(u, v)} e^{i(k_x u + k_y v)} du dv \quad (2.24)$$

$$= \mathcal{F} \left\{ A(u, v) e^{-\frac{2\pi i}{\lambda} \Delta W(u, v)} \right\}. \quad (2.25)$$

Note that in the last step we have simply inserted the definition of the two-dimensional Fourier transform. The amplitude of the electric field at point P is thus given by the Fourier transform of product of the aperture function and the exponential term corresponding to the aberrations. Omitting the aberrations, i. e. considering ideal wavefronts, would lead to the well-known airy disk.

2.3 Spatial Filtering of Aberrated Wavefronts

Consider the so-called $4f$ -system illustrated in Figure 2.2. The input plane is equivalent to the aperture plane in illustration 2.1 and contains the aperture with aperture function $A_1(u, v)$. Adding a pinhole in the Fourier plane with aperture function $A_2(k_x, k_y)$ results in the final amplitude of the aberrated electric field in the image plane being a convolution of the first aperture function and the inverse Fourier transform of the second one, i. e.

$$E(x, y) = \left(A_1(u, v) e^{-\frac{2\pi i}{\lambda} \Delta W(u, v)} \right) * \mathcal{F}^{-1} \{ A_2(k_x, k_y) \} \quad (2.26)$$

$$= \mathcal{F}^{-1} \left\{ \mathcal{F} \left\{ A_1(u, v) e^{-\frac{2\pi i}{\lambda} \Delta W(u, v)} \right\} \cdot A_2(k_x, k_y) \right\}, \quad (2.27)$$

where in (2.27) we have used that the convolution of two functions is equal to the inverse Fourier transform of the product of the Fourier transforms of the two functions. Note that $A_2(k_x, k_y)$ is similarly defined to $A_1(u, v)$, but in the frequency domain.

2.4 Null Depth

In nulling interferometry, two beams as given by equation (2.27) are constructively (+) and destructively (-) superimposed. In this work, one of the two beams will be treated

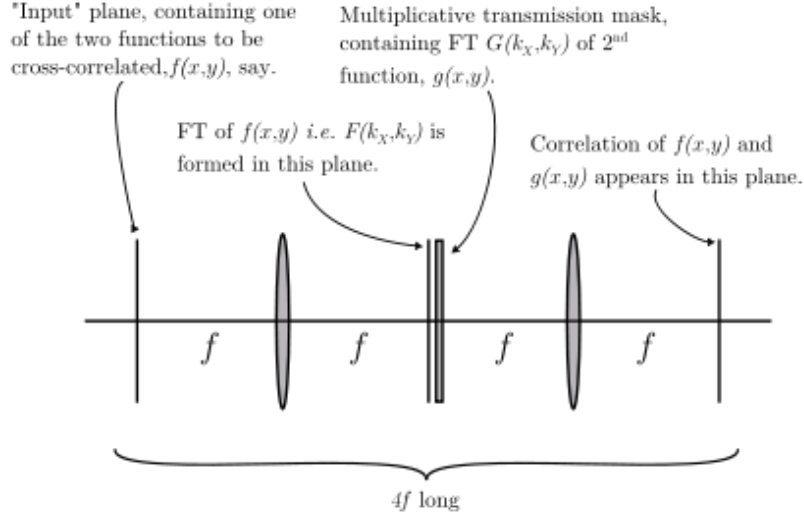


Figure 2.2: Illustration of the $4f$ -system setup.

as ideal, i. e. without aberrations. This yields the total amplitudes

$$E_+(x, y) = E_{\text{ideal}}(x, y) + E_{\text{aberrated}}(x, y), \quad (2.28)$$

$$E_-(x, y) = E_{\text{ideal}}(x, y) - E_{\text{aberrated}}(x, y). \quad (2.29)$$

This results in the two intensities (neglecting some constants)

$$I_+(x, y) = |\mathcal{R}(E_+(x, y))|^2, \quad (2.30)$$

$$I_-(x, y) = |\mathcal{R}(E_-(x, y))|^2, \quad (2.31)$$

where $\mathcal{R}(\cdot)$ denotes the real part of the complex amplitudes. With this we can now define the null depth as

$$N(x, y) = \frac{I_-(x, y)}{I_+(x, y)}. \quad (2.32)$$

2.5 Throughput

The total initial intensity of the combined ideal and the aberrated wavefronts is given by

$$I_{\text{init}}(u, v) = \left| \mathcal{R} \left(A_{0,\text{id}} + A_{0,\text{ab}} e^{-\frac{2\pi i}{\lambda} \Delta W(u, v)} \right) \right|^2, \quad (2.33)$$

where $A_{0,i}$ is defined as in (2.19). In this particular work, the throughput is then defined as the ratio of the final intensity $I_+(x, y)$ of the combined wavefronts as given in (2.30) and $I_{\text{init}}(x, y)$, i. e.

$$T(x, y) = \frac{I_+(x, y)}{I_{\text{init}}(x, y)}. \quad (2.34)$$

3 Methodology

3.1 Normalization

In this work, the initial amplitudes $A_{0,\text{id}}$ and $A_{0,\text{ab}}$ are chosen such that the total initial intensity of the combined ideal and aberrated wavefronts as given in (2.33) is unity, i. e.

$$I_{\text{init}}(u, v) = 1. \tag{3.1}$$

4 Results

5 Discussion

6 Conclusion

References

Abhijit Patil, Rajesh Langoju, and Pramod Rastogi. Signal-processing methods in phase-shifting interferometry. *Phase Estimation in Optical Interferometry*, XI:235–272, 2014. doi: 10.1201/b17701.

Appendices